EUROPEAN COMMISSION

European Research Area

D5.1 and D5.2 – Literature Review and First Year Synthesis and preliminary report on consequences of solubility uncertainties

SLOW PROCESSES IN CLOSE-TO-EQUILIBRIUM CONDITIONS FOR RADIONUCLIDES IN WATER/SOLID SYSTEMS OF RELEVANCE TO NUCLEAR WASTE MANAGEMENT

SKIN

COLLABORATIVE PROJECT (CP)

Reporting period: 01/01/2011-31/12/2013

Grant agreement N°.: FP7-269688

Submitting organizations: AMPHOS and ARMINES
Due date of deliverable: Project Month 14
Actual submission: Project Month 18

Start date of the project: 01 January 2011
Duration: 36 months

Project co-funded by the European Commission under the Seventh Framework Programme of the European Atomic Energy Community (Euratom) for nuclear research and training activities (2007 to 2011)		
Dissemination Level		
PU	Public	X
RE	Restricted to a group specified by the partners of the project	
CO	Confidential, only for partners of the project	

EURATOM

1. Introduction

High uncertainties in the solubility of some elements may result in high uncertainties in the results of the calculations used to support of safety assessments. A safety assessment is performed to evaluate the impact of the SKIN project in reducing the uncertainties on solubility values.

The main objective of the work package 5 of the SKIN project is to provide an overall synthesis of the project results together with results of previous studies (literature and field data). The goals of this deliverable are the following ones:

- To present the conceptual safety assessment model
- To provide a literature review on thorium solubility
- To show preliminary results

This exercise requires the development of a model based on geological disposal of radioactive waste. A performance assessment reference case is described to undertake that task. First of all, the PA model will be used with data already in literature as a starting point. At the end of the project, the solubility and sorption parameters will be changed according to the improvements achieved in SKIN. Finally, a comparison of both cases will be done to evaluate the contribution of SKIN in this field.

It will be used the compartmental code AMBER© to build up an integrated source term model for the performance assessment of spent fuel under repository conditions. This model describes the radionuclide release from spent nuclear fuel, disposed in a deep geological disposal, to both near and far field.

The present deliverable is composed of three main sections according with the aims of it:

- Chapter 2: The Performance Assessment Case: description of the model and its implementation in the Amber© code
- Chapter 3: Solubility review: literature review of thorium solubility data
- Chapter 4: Results: preliminary results of the PA model using data from literature

2. PA case description

The PA case used for the evaluation of the achievements of the SKIN project is based on the Swedish SR-Site exercise. Spent fuel from Swedish nuclear power plants are managed by SKB (Swedish Nuclear Fuel and Waste Management Company) and are planned to be placed into a deep geological repository. KBS-3 is the disposal concept followed in that study.

KBS-3 concept (Figure 1) consists on the disposal of the spent nuclear fuel in cooper canisters with a cast iron insert surrounded by bentonite clay. All this system is host in a granitic rock formation at approximately 500m depth (SKB 2011). The disposal is based on a multibarrier design where the UO_2 pellet itself works as the first engineered barrier. The following ones are the bentonite and the altered granite called as EDF (*Excavation Damaged Zone*), which are part of the near field and their functionality is to avoid the arrival of radionuclides to far field (non-altered granite).

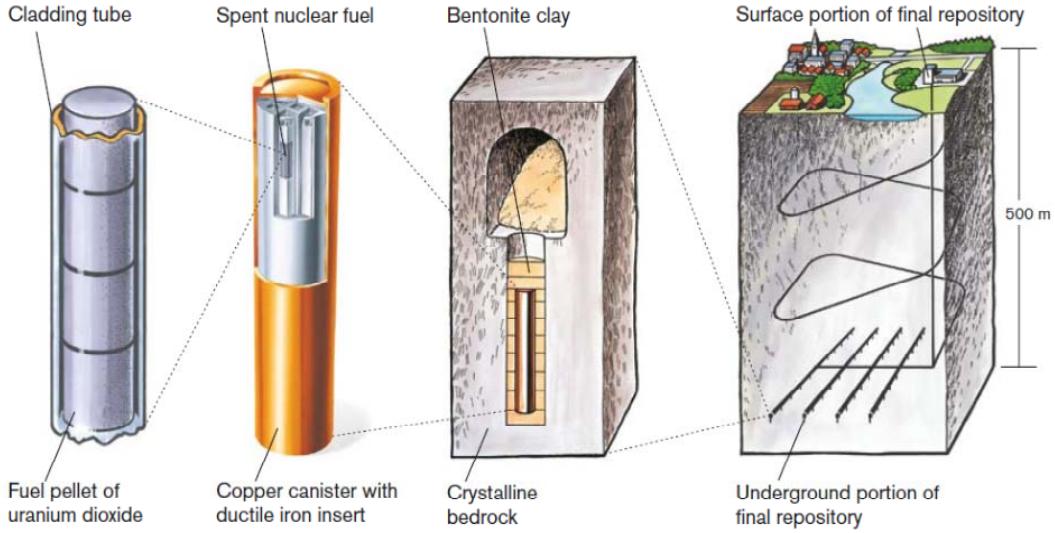

Figure 1: The KBS-3 concept for disposal of spent nuclear fuel (SKB 2011)

It is assumed that groundwater will reach the waste after around 50,000 years, when it is supposed that the canister failure will occur. At that time, radionuclides present in the gap and grain boundaries are instantaneously released to the bentonite clay. Radionuclides embedded in the UO_2 matrix are progressively released in a congruent way with the oxidative dissolution of the matrix. From bentonite, contaminants are moved to granite rock by diffusive processes and afterwards, they migrate through the granite media by advection until scape from the system.

As mentioned before, the Swedish concept is represented as a compartmental model able to be implemented in the Amber© code. The model has been build up following the information provided from SKB reports such as the Main report of the SR-Site (SKB 2011) or the Data report for the safety assessment (SKB 2010a).

The following sub-sections deal with the presentation of the code to be used (Amber©) and the compartmental model that describes the KBS-3 system.

2.1 Amber© code

The compartmental code Amber© (Quintessa Limited 2011) is commonly used to study the transport of trace elements through complex systems. The system is divided in several components called compartments which are connected to each other by mass transfer fluxes. It is a flexible program where all processes affecting radionuclide mobility can be implemented (e.g. advection, diffusion, erosion, sorption…). In addition, Amber© allows considering decay of radionuclides with time.

Before performing the compartmental model, it is important to keep in mind the following aspects regarding the program functionalities:

- All species are at trace level, thus they do not modify the characteristics of the compartments
- The species are homogeneously distributed in each compartment
- Transfer between compartments is described by first order rates. Each transfer is 'donor controlled', depending directly on the amount of the element present in the compartment from which the material is moving to

The amount of the species in each compartment is determined by the Equation 1 and it could be expressed in terms of moles of substance, mass or activity (i.e. mol, kg, Bq, respectively). All the transport parameters should be defined as well as the decay constants.

$$\frac{dI_i^m}{dt} = -\left[\lambda_r^m + \sum_j \lambda_{ij}\right] \cdot I_i^m + \lambda_r^{m+1} \cdot I_i^{m+1} + \sum_j \lambda_{ji} \cdot I_j^m \qquad \textbf{Equation 1}$$

Where,

λ_r^m decay rate of radionuclide *m* (y^{-1})

λ_r^{m+1}	decay rate of the parent radionuclide *m+1* (y^{-1})
λ_{ij}	exchange rate between compartment *i* and compartment *j* (y^{-1})
λ_{ji}	exchange rate between compartment *j* and compartment *i* (y^{-1})
I_i^m	amount of species *m* in compartment *i* (mol, kg, Bq)
I_i^{m+1}	amount of species *m+1* in compartment *i* (mol, kg, Bq)
I_j^m	amount of species *m* in compartment *j* (mol, kg, Bq)

2.2 Model description

This section presents the steps required to build up the compartmental model developed on the basis of the Swedish repository concept in Amber©. The methodology is divided into 6 steps:

1. Contaminants: definition of the radionuclides of interest in the safety assessment including decay chains and the associated data
2. Compartments: description of the components of the system that should be considered
3. Transferences: determination of transferences between compartments and other processes that may affect the mobility of radionuclides. Formulation of the transfer rates is also provided.
4. Parameters: selection of required data for each parameter defined in previous steps
5. Result time: citation of the times when the model will obtain output results
6. Calculation: obtaining of outcome results

Following, more detailed information regarding each of the above steps is exposed.

STEP 1. Contaminants: Isotopes and decay chains

Amber© defines contaminants as trace elements which evolution in compartments is of interest. Their presence does not affect the characteristics of the system. In the present assessment, contaminants are referred to radionuclides that can be found in the spent nuclear fuel. Specifically, radionuclides of interest in that study are the ones treated in the frame of SKIN.

Table 1 lists the elements of interest and the isotopes of each element considered in the present assessment. In the model it is introduced the decay of all radionuclides and in

the case on the ones which are part of a natural decay chain (^{238}U, ^{235}U and ^{232}Th), all the chain is considered. For that reason, some elements not treated in the SKIN project are introduced in the model (radionuclides in grey in Table 1). Radioactive decay processes is not only considered in the waste (spent fuel) but also during radionuclide migration through all the system.

Table 1: Radionuclides of interest

Element	Isotopes
Ac	^{228}Ac, ^{227}Ac
Am	^{241}Am
Cs	^{137}Cs
Eu	^{152}Eu
Np	^{237}Np
Pa	^{234m}Pa, ^{231}Pa
Ra	^{228}Ra, ^{226}Ra, ^{224}Ra, ^{223}Ra
Se	^{79}Se
Sr	^{90}Sr
Tc	^{99}Tc
Th	^{234}Th, ^{232}Th, ^{231}Th, ^{230}Th, ^{228}Th, ^{227}Th
U	^{238}U, ^{235}U, ^{234}U

Decay chains considered in that assessment as well as the associated decay data (i.e. half-lives) is presented in the Appendix (Table 4).

STEP 2. Compartments

A compartment is a distinct physical entity (e.g. soil, host rock, river, waste…) through which contaminants may pass and/or in which contaminants may accumulate. It is assumed instantaneous mixing within a given compartment.

The system used for the reference case has been divided into 6 main compartments (Figure 2): waste, canister, bentonite, altered granite (EDZ), non-altered granite and sink. The last compartment represents the surroundings of the system. The radionuclides released in the sink compartment are assumed to escape the defined system.

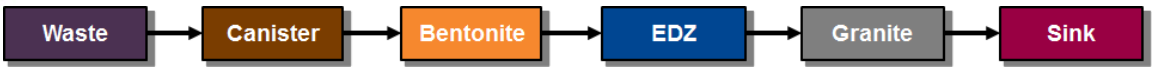

Figure 2: Compartments considered in the reference model

Bentonite and granite compartments are split into 5 sub-compartments each of them, trying to improve the results and to avoid numeric dispersion.

Characteristics of each compartment are presented in the Appendix where volumes, porosity or densities are described. The initial amount of 'contaminants' is set to zero in all the compartments except for the waste compartment. The inventory of spent fuel is obtained from SKB (2010a) where it is provide the average inventory at year 2045 recommended using in SR-Site.

STEP 3. Transferences

Transferences are the processes by which contaminants can move from a donor to a receptor compartment. The transfer flux is the amount of a given contaminant flowing between two compartments per unit time. It is obtained multiplying the amount in the donor compartment by the transfer rate.

Transfer processes between compartments are defined taking into account physic and chemical characteristics of the system. In that assessment the radionuclide fluxes are result of: instant release, matrix dissolution, advection and diffusion (Figure 3).

Two transfer mechanism are introduced from spent fuel to gap water, i.e. IRF and matrix dissolution. Instant release fraction only applies for radionuclides accumulated in gap and grain boundaries. It represents the fraction of the total radionuclide inventory that is modelled to be instantly released to the interior of the canister when water reaches the spent fuel. That release only occurs during the first year after the contact of water with the waste.
Exchange rate (see Equation 1) regarding the instant release fraction is calculated as Equation 2 shows.

$$\lambda_{IRF} = -ln(1 - IRF) \qquad \textbf{Equation 2}$$

IRF Fraction of RN instantly released (-)

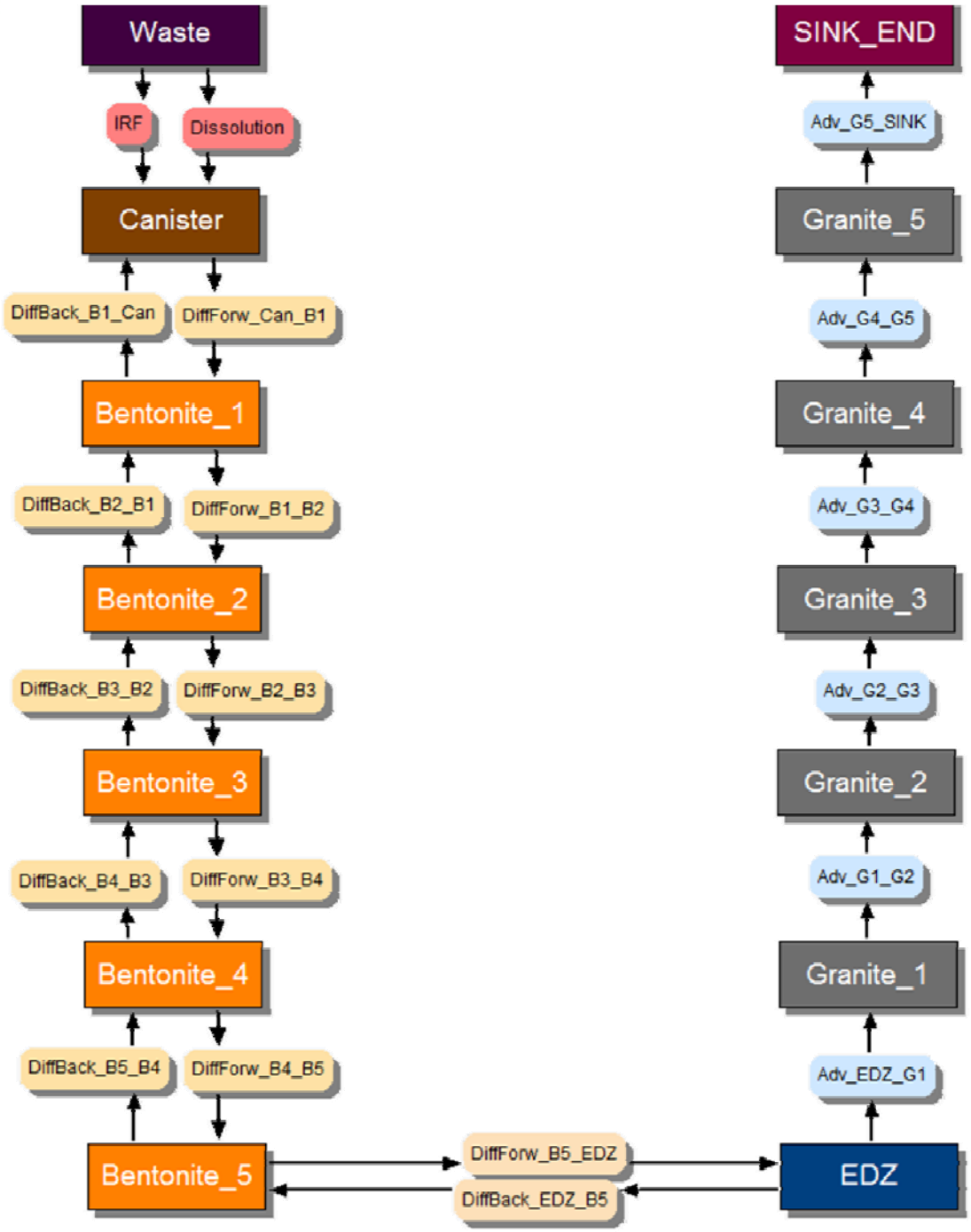

Figure 3: Scheme of compartiments and transferences considered in the reference model

Oxidative dissolution of UO_2 matrix occurs slower than IRF but it occurs longer in time. It is considered a congruent dissolution, so, all radionuclides embedded in the matrix are mobilized at the same rate than uranium.

After the radionuclides come into the canister compartment, their transport through the bentonite is mainly by diffusion. The diffusion process between two compartments is represented by two processes to overcome the Amber© limitation that transfer fluxes are only dependent of the amount of donor compartment.

1. Forward transfer: transfer from the donor (*i*) to the receiving (*j*) compartment
2. Backward transfer: transfer from the receiving (*j*) to the donor (*i*) compartment

In Equation 3 it is shown how to calculate the forward diffusion transfer rate for element *m* (form compartment *i* to compartment *j*). The same equation is used for backward diffusion changing the order of compartments (from compartment *j* to compartment *i*). It is introduced the effective diffusion coefficient (D_e), to take into account the mechanism of anion exclusion.

$$\lambda_{ij,m}^{diff} = \frac{D_{ij,m} \cdot S_{ij}}{\theta_{i,m} \cdot R_{i,m} \cdot V_i \cdot \Delta_{ij}} \qquad D_{ij,m} = \frac{\Delta_{ij}}{\frac{\Delta_i}{D_{e,i,m}} + \frac{\Delta_j}{D_{e,j,m}}}$$

Equation 3

$$S_{ij} = L_i \cdot \pi \cdot r_{ij}$$

$$\theta_{i,m} = \theta_i \cdot f_{i,m}$$

$$R_{i,m} = 1 + \frac{(1 - \theta_{i,m}) \cdot \rho_i \cdot K_{d,i,m}}{\theta_{i,m}}$$

S_{ij}	Surface area between compartments *i* and *j* (m^2)
$L_i \cdot$	Length of compartment *i* (m)
r_{ij}	External radius of compartment *i* = Internal radius of compartment *j* (m)
V_i	Total volume of compartment *i* (m^3)
Δ_{ij}	Diffusion length between compartments *i* and *j* (m)
$D_{ij,m}$	Diffusion factor for the transport of *m* between compartments *i* and *j* (m^3/s)
Δ_i	Diffusion length of compartment *i* (One half of the width of compartment *i*) (m)
$D_{e,i,m}$	Effective diffusion coefficient of *m* in compartment *i* (m^2/s)

$R_{i,m}$ Retardation factor of *m* in compartment *i* (-)

$\theta_{i,m}$ Accessible porosity of *m* in compartment *i* (-)

ρ_i Density of compartment *i* (kg/m^3)

$K_{d,i,m}$ Distribution coefficient of *m* in compartment *i* (m^3/kg)

Once radionuclides reach the EDZ, their transport is result of water fluxes. Thus, advection is the mechanism by which contaminants are moving through the granite media until escape the system entering into the sink compartment. The advective transport is represented as in Equation 4.

$$\lambda_{ij,m}^{adv} = \frac{Q}{\theta_{i,m} \cdot R_{i,m} \cdot V_i}$$ **Equation 4**

Q Water flow in compartment *i* (m^3/y)

As well as the transfer processes described above, there are other phenomena controlling the mobility of radionuclides integrated into the model. Maximum concentration of the elements in the compartments is expected to be controlled by their solubility. In the code, solubility is implemented as a transfer limitation. That means that the amount of an element (sum of all isotopes of that element) transferred from one to other compartment is limited by solubility. Equation 5 shows how the transfer limit for an element *e* is calculated considering that may be controlled by solubility.

$$Limit_{ij,e} = SolLim_{e,i} \cdot V_i \cdot \theta_i \cdot R_{m,i}$$ **Equation 5**

$SolLim_{e,i}$ Solubility of element *e* in compartment *i* (mol/L)

The transference of a radionuclide from the donor to the receptor compartment is modelled as shown in Equation 6. Transfer rate from *i* to *j* not only is multiplied by the amount of the radionuclide in the donor compartment but also by a dimensionless parameter standing for the availability.

$$Transfer\ Flux_{ij,m} = \lambda_{ij,m} \cdot Availability_{ij,e} \cdot Amount_{m,i}$$ **Equation 6**

$\lambda_{ij,m}$ Transfer rate from compartment *i* to compartment *j* (y^{-1})

$Availability_{ij,e}$ Availability of element *e* to be transferred from *i* to compartment *j* (-) (see Equation 7)

$Amount_{m,i}$ Amount of radionuclide *m* in donor compartment (mol)

The availability term is where solubility limitation is taken into account (Equation 7). That parameter ranges from 0 to 1. The unity means that all radionuclide in donor compartment can be transferred, thus its concentration is lower than the solubility limit (Limit/amount > 1). But if the concentration of the element is higher than the solubility limit, solid phases precipitates, and so, not all its amount is available to be transferred. In that case, the availability parameter takes the value of the fraction between the limit and the amount.

$$Availability_{ij,e} = min\left(\frac{Limit_{ij,e}}{Amount_{e,i}}, 1\right)$$ **Equation 7**

STEP 4. Parameters

All parameters and data required for the implementation of the reference case into Amber© are presented in the Appendix.

STEP 5. Result times

Before the model is run, it is important to define to which times the results should be analysed. Taking into account that the objective of this project is based on solubility and sorption parameters, it is not useful to look at the behaviour of the system during the period before the canister failure (0 to 50,000). Therefore, output data of interest will be extracted at the following times: $5 \cdot 10^4$, $8 \cdot 10^4$, $1 \cdot 10^5$, $3 \cdot 10^5$, $5 \cdot 10^5$, $8 \cdot 10^5$ and $1 \cdot 10^6$ years.

STEP 6. Calculation

Once all previous steps (1 to 5) are done, the model is completely implemented in the software and could be calculated. Output parameters of interest are the concentration in molarity or activity of each element en each compartment. Results when running the model with literature data are presented in section 4. In further reports, solubility and sorption data obtained in the frame of the SKIN project will be implemented in the present model. Results will be compared with the ones of the reference case to analyse the contribution of this project on reducing uncertainties in that kind of assessments.

3. Review of solubility measurements and assessment

The solubility of thorium oxide and/or its hydroxide forms has been studied for many years. The solids are denoted differently in the literature and there is a lack of thorough solid-state analyses. Typically XRD analyses note the "absence of an XRD pattern". This is not sufficient to unambiguously characterize solids. Table 2 presents Th-based solids used in the various solubility studies in the literature. These studies are grouped in the present report by defining two sets of solids with respect to the crystalline state, the hydroxylation and hydration rate: 1) crystallized thorium oxide synthesized at high temperature with a fully crystalline state as confirmed by XRD analyses (denoted as "ThO_2(cr)"); 2) a thorium hydroxide with an hydrous and hydroxyl component ("$ThO_x(OH)_y(H_2O)_z$(am)"). In the following, various solubility studies are discussed for each group. Results of these solubility studies are reproduced in Figure 4.

1. ThO_2(cr): In most cases for the studies discussed in this group, experimental conditions were not strictly controlled to obtain fully crystallized solids and most of them were not characterized by XRD. The synthesis conditions for obtaining ThO_2(cr) are: 1) a slow precipitation with a nitrate or an oxalate precursor; 2) and heating at 700°C for a few days (Hubert et al. 2001). The solids studied in all works (Hubert et al. 2001; Heisbourg 2003; Rai et al. 2000) were synthesized at high temperature (T=750°C) and characterized as fully crystallized solids by XRD. However, the solubility values reported (Hubert et al. 2001; Heisbourg 2003) in Figure 4, either from an undersaturated experiment (dissolution) using ThO_2(cr) or from over-saturated conditions (precipitation), result in a non-identified, probably amorphous solid. This may explain the observed differences in solubilities. The other solids named ThO_2(cr) are commercially available (Altmaier et al. 2004; Rothe et al. 2002) or sintered spheres fuel for HTR (High Temperature Reactor) (Landesman et al. 2004; Vandenborre et al, 2008).

2. $ThO_x(OH)_y(H_2O)_z$(s): This group corresponds not to one solid but to a whole class of different solids. Solid phases in this group are typically obtained by quick precipitation by NaOH addition to an aqueous solution of a nitrate precursor, followed by water washing without heating. In most cases the experimental synthesis conditions are not detailed in the literature (Rai et al. 2000; Felmy et al. 1991; Moon 1989; Nabivanets and Kudritskaya 1964; Rai et al. 1997; Ryan and Rai 1987). Hence, surface properties are not precisely defined for the obtained solid. Thus, we assume that the studied solids are quite different from one author to another, because they depend on the synthesis

conditions (precipitation rate, drying time, pH of the media) as indicated by the review of Rand et al. (2008). The amorphous character is often only "identified" by noting the absence of an X-ray diffraction pattern, but amorphous solids may well be nano-cristalline as evidenced by electron diffraction. The crystalline/amorphous state was in some cases not studied at all (Moon 1989), but there are also detailed studies, where electron diffraction analysis (Baes et al 1965; Bundschuh et al. 2000) and TEM (transmission electron microscopy) techniques have been undertaken. These studies have shown that, for solids precipitated from supersaturated conditions, very small ThO_2(cr) crystallites (1-10 nm) were scattered in an amorphous phase (Dzimitrowicz et al. 1985; Rousseau et al. 2002; Rousseau et al. 2006). Hence, the notation of "$ThO_x(OH)_y(H_2O)_z$(s)" covers many cases: 1) synthesized solids which are dried for a sufficiently long time (one week at T=25°C) to obtain a partial crystallization and which are named "microcrystallized" by the authors (Rai et al. 2000; Moon 1989; Dzimitrowicz et al. 1985; Jernström et al. 2002; Neck et al. 2002; Östhols 1995; Östhols et al. 1994; Wierczinski et al. 1998); 2) other solids which have been precipitated from over-saturated conditions (Baes et al 1965; Rousseau et al. 2002; Rousseau et al. 2006; Heisbourg et al. 2003) show solubility values close to those of colloidal particles measured by LIBD (laser induced breakdown detection) (Altmaier et al. 2004; Bundschuh et al. 2000; Neck et al. 2002; Altmaier et al. 2005; Bitea et al. 2003).

For some authors (Rai et al. 2000; Rand et al. 2008), the crystallization rate was suggested as an important parameter controlling the solubility of Th-solids. The higher the crystallization rate the lower the solubility values (cf. $ThO_x(OH)_y(H_2O)_z$(s) data (Rai et al. 2000) in Figure 4). Other authors (Östhols 1995; Östhols et al. 1994) have shown that the specific surface area values, measured by B.E.T., strongly depend on the conditions of synthesis of the solid sample ($16<$Surface Area<76 $m^2.g^{-1}$). At atomic scale, EXAFS analysis shows that commercial ThO_2(cr) and colloidal particles display different Th chemical environments (Rothe et al. 2002). Most authors assume that the solubility properties of the solids are linked to surface phenomena (Felmy et al. 1991; Rand et al. 2008; Neck et al. 2001). A recently published work (Rand et al. 2008) sheds some light on the difficulty in performing realistic solubility experiments with ThO_2. They indicate that many authors have spent insufficient effort in separating solid and aqueous phases. Measured Th concentrations were often higher because colloidal particles and/or polynuclear species were not sufficiently filtrated. The authors (Rand et al. 2008) underline that solubility is not controlled by the solid bulk but rather by amorphous or non-identified microcrystalline surface phases. Moreover they notice that the published studies have been carried out using Th hydroxide phases within a large range of particle size, caused by varying synthesis conditions and ageing times. Using four sets of particle size: >30 nm, 10-30 nm, 5-10 nm and <5 nm (measured by an independent method) and by determining surface energy contributions to the solubility

they propose an explanation in the discrepancy in thorium solubility values. The work presented here tries to bring to a whole this point of view.

To conclude, Figure 4 shows three sets of solubility values are linked to two kinds of solids: 1) solid $ThO_x(OH)_y(H_2O)_z(s)$ with high solubility values (1 10^{-2} mol.l^{-1} for pH=4.5); 2) solid $ThO_2(cr)$ with low solubility values (1 10^{-7} mol.l^{-1} for pH=2.5); 3) a solid that is not clearly identified with a broad range of intermediate solubility values (between 1 10^{-2} mol.l^{-1} and 1 10^{-6} mol.l^{-1} for pH=3.5). The corresponding variation in solubility products is presented in

Table 3, using, for both solids, the formal stoichiometric reactionEquation 8:

$$ThO_2 + 2H_2O \leftrightarrow Th^{4+} + 4OH$$ **Equation 8**

The solubility product values range between $ThO_2(cr)$ (log K°sp=-56.9 (Rai et al. 2000) and $ThO_x(OH)_y(H_2O)_z(s)$ (log K°sp=-45.5 (Felmy et al. 1991; Rai et al. 1997) while an average value was suggested for the amorphous phase (Bitea et al. 2003) (log K°sp=-47). Moreover, a difference has been established (Rai et al. 1997) between freshly prepared hydroxide (log K°sp=-46.7) and the aged phase (log K°sp=-47.5). A solubility product has been calculated from thermodynamic data, derived from calorimetric experiments (log K°sp=-54.2 (Cox et al. 1989; Fuger and Oetting 1976; Wagman et al. 1982) for $ThO_2(cr)$. However, authors (Rand et al. 2008) have suggested that the formation of OH groups on the surface modifies the solubility of $ThO_2(cr)$ when compared to solubility values calculated from microcalorimetric measurements. However, most oxides, like for example SiO_2, form OH groups at the surface but this does not lead to discrepancy between solid state thermodynamic data and thermodynamic data obtained from solubility values. Hence, despite the careful recent review of thermodynamic data (Rand et al. 2008) it is still not clear how to predict thorium oxide solubility. Therefore, the large uncertainty in solid phase properties and solubility product values requires a new approach linking bulk solid, solid surface and solubility properties. We use solid analysis, leaching experiment and isotopic exchange to contribute to the understanding of the discrepancy in the solubility data and to describe the degree of reversibility in exchange mechanisms.

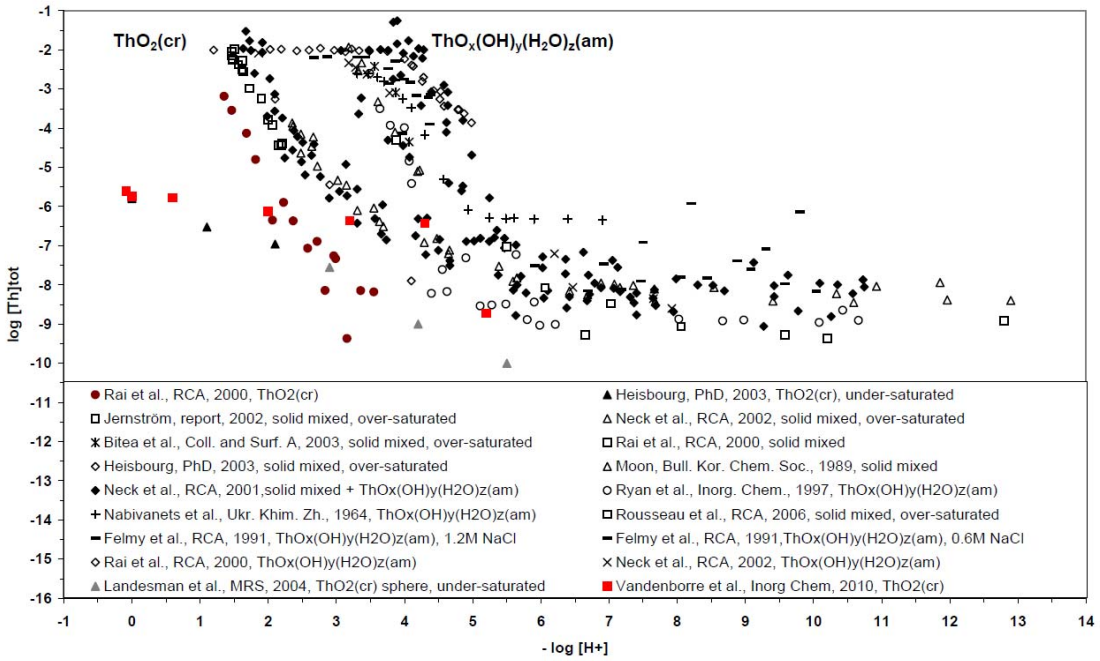

Figure 4: Solubility values from literature

Table 2: Data from literature about thorium oxide names

Publications	Name in paper	Solid characterization	Name chosen in this work
Rai et al. (2000) Altmaier et al. (2004) Rothe et al. (2002)	ThO_2(cr)	XRD	ThO_2(cr)
Landesman et al. (2004) Vandenborre et al. (2008) Heisbourg (2003) Hubert et al. (2001)		XRD	
Dzimitrowicz et al. (1985) Neck et al. (2001) Östhols (1995) Östhols et al. (1994) Rai et al. (2000) Rothe et al. (2002) Wierczinski et al. (1998)	ThO_2 (microcr)	XRD, BET, electronic diffraction	$ThO_x(OH)_y(H_2O)_z$ (s)
Moon (1989) Neck et al. (2001)		no	
Baes et al (1965) Bitea et al. (2003) Bundschuh et al. (2000) Heisbourg (2003) Jernström et al. (2002) Neck et al. (2001) Neck et al. (2002) Rothe et al. (2002) Rousseau (2002) Rousseau et al. (2006) Ryan and Rai (1987)	ThO_2(coll) or $ThO_n(OH)_{4-2n}xH_2O$	XRD, electronic diffraction, EXAFS, TEM	
Altmaier et al. (2004) Altmaier et al. (2005) Felmy et al. (1991) Moon (1989) Nabivanets and Kudritskaya (1964) Neck et al. (2002) Neck et al.(2001) Rai et al. (1997) Rai et al. (2000) Rothe et al. (2002) Ryan and Rai (1987)	$ThO_2.xH_2O$, ThO_2(am) or $Th(OH)_4$(am)	XRD	

Table 3: Solubility product values from literature

Solid	log K°$_{sp}$ exp	Publications
$ThO_x(OH)_y(H_2O)_z(s)$	-53.2	Rothe et al. (2002)
	-49.2	Rai et al. (2000)
	-52.8	Bundschuh et al. (2000)
	-48.7	Östhols et al. (1994)
	-47	Neck et al. (2001)
	-52.9	Moon (1989) Neck et al. (2002)
	-47.8	Neck et al. (2002)
	-46.6	Moon (1989)
	-45.5	Felmy et al. (1991)
	-45.5	Rai et al. (1997)
	-47.3	Ryan and Rai (1987)
	-46.6	Nabivanets and Kudritskaya (1964) Baes et al (1965)
	-46.2	Rai et al. (2000)
ThO_2(cr)	-56.9	Rai et al. (2000)

4. Results of the reference case

In this section, it is presented the results obtained from the implementation of the reference case based on SKB repository concept. That data will be used in further steps as a reference to compare with results obtained after the implementation of new data coming from SKIN project studies.

Figure 5 shows the concentration of the elements of interest in the first and last compartments of bentonite and granite. Americium, caesium, europium and strontium are not represented in the graphs due to the short half-lives of their isotopes (see Table 4 in the Appendix).

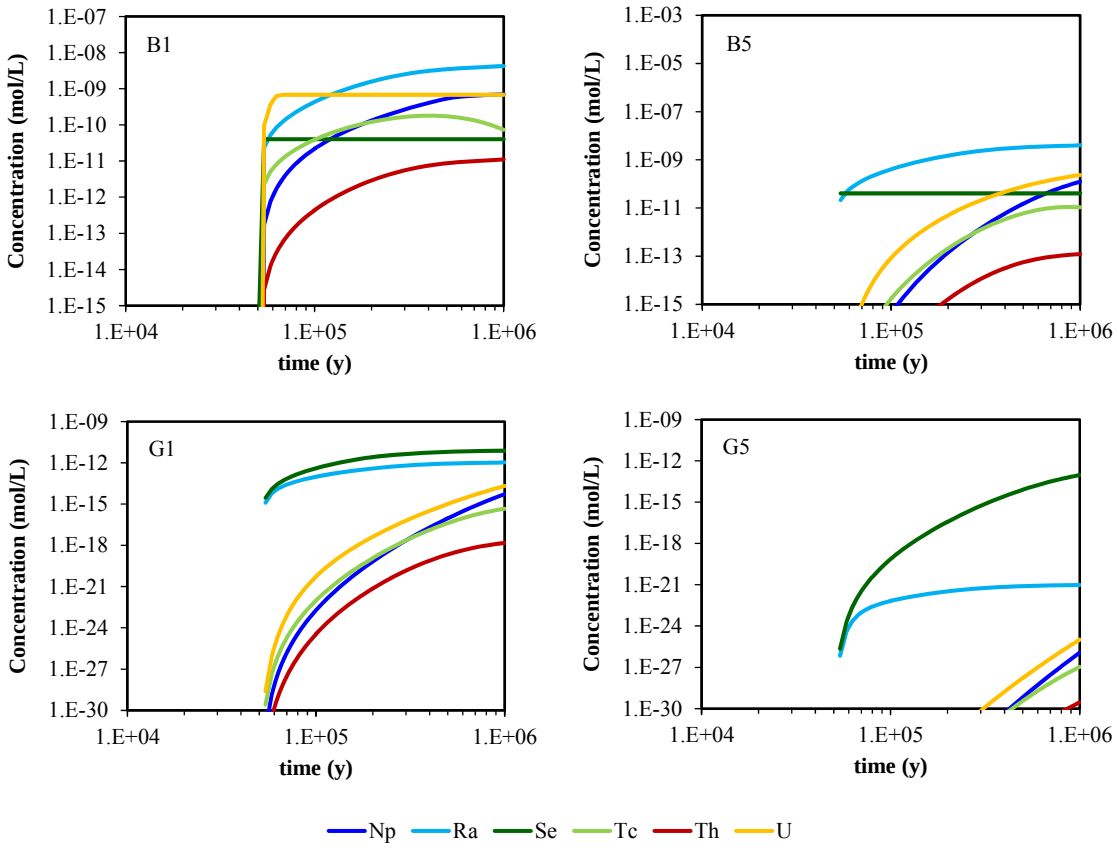

Figure 5: Concentration of Np, Ra, Se, Tc, Th and U in compartments B1 (top left), B5 (top right), G1 (bottom left) and G5 (bottom right)

In previous section, a literature review of thorium solubility has been done. It has been provided a range of solubility values to use according with the amorphous phase of ThO_2 ($7.9 \cdot 10^{-9}$ – $1.3 \cdot 10^{-9}$ mol/L). However, a maximum value of $1.3 \cdot 10^{-7}$M is published in some studies. In the model, thorium solubility in the canister and bentonite is $7.9 \cdot 10^{-7}$M and in granite is $8.9 \cdot 10^{-9}$M. Those values are in agreement with literature data. The concentration of thorium in all compartments from bentonite to granite is shown in Figure 6.

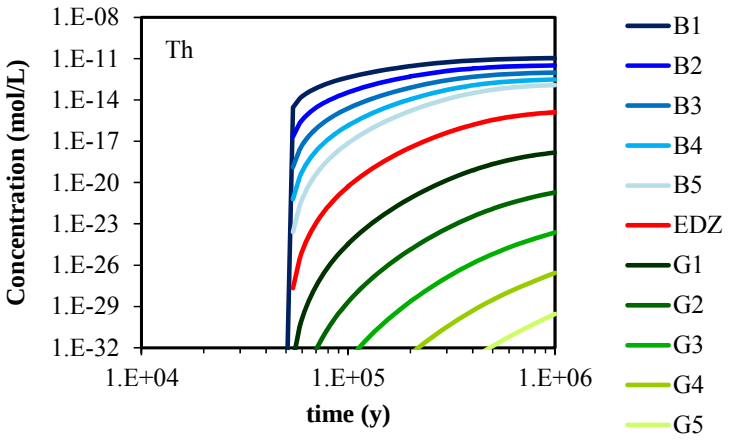

Figure 6: Thorium concentration in all compartments of the System from the first one of bentonite to the last of granite

5. References

Altmaier, M., Neck, V., Fanghänel, Th. (2004) Solubility and colloid formation of Th(IV) in concentrated NaCl and $MgCl_2$ solution. Radiochim. Acta, 92, 537-543

Altmaier, M., Neck, V., Müller, R., Fanghänel, Th. (2005) Solubility of $ThO_2.xH_2O$(am) in carbonate solution and the formation of ternary Th(IV) hydroxide-carbonate complexes. Radiochim. Acta, 93, 83-92

Baes, C.F., Meyer, N.J., Roberts, C.E. (1965) The Hydrolysis of Thorium(IV) at 0 and 95°. Inorg. Chem., 4, 518-527

Bitea, C., Müller, R., Neck, V., Walther, C., Kim, J.I. (2003) Study of the generation and stability of thorium(IV) colloids by LIBD combined with ultrafiltration. Colloids Surf., A, 217, 63-70

Bundschuh, T., Knopp, R., Müller, R., Kim, J.I., Neck, V., Fanghänel, Th. (2000) Application of LIBD to the determination of the solubility product of thorium (IV)-colloids. Radiochim. Acta, 88, 625-629

Cox, J.D., Wagman, D.D., Medvedev, V.A. (1989) CODATA Key Values for Thermodynamics. book. Hemisphere Pub. Corp. 271

Duro, L., Grivé, M., Cera, E., Gaona, X., Domènech, C., Bruno, J. (2006) Determination and assessment of the concentration limits to be used in SR-Can. SKB Technical Report, TR-06-32

Dzimitrowicz, D.J., Wiseman, P.J., Cherns, D. (1985) An electron microscope study of hydrous thorium dioxide $ThO_2.nH_2O$. J. Colloid Interface Sci., 103, 170-177

Felmy, A.R., Rai, D., Mason, M.J. (1991) The solubility of hydrous thorium(IV) oxide in chloride media : development of an aqueous ion-interaction model. Radiochim. Acta, 55, 177-185

Fuger, J., Oetting, F.L. (1976) The Chemical Thermodynamics of Actinide Elements and Compounds : Part 2, The Actinide Aqueous Ions. book, ed. IAEA.

Grivé, M., Domènech, C., Montoya, V., García, D., Duro, L. (2010) Determination and assessment of the concentration limits to be used in SR-Can. Supplement to TR-06-32. SKB Report, R-10-50

Heisbourg, G. (2003) Synthèse, caractérisation et études cinétique et thermodynamique de la dissolution de ThO_2 et des solutions solides $Th_{1-x}M_xO_2$ (M = U, Pu), in Ph.D. Université Paris XI: Orsay

Heisbourg, G., Hubert, S., Dacheux, N., Ritt, J. (2003) The kinetics of dissolution of $Th_{1-x}U_xO_2$ solid solutions in nitric media. J. Nucl. Mater., 321, 141-151

Hubert, S., Barthelet, K., Fourest, B., Lagrade, G., Dacheux, N., Baglan, N. (2001) Influence of the precursor and the calcination temperature on the dissolution of thorium dioxide. J. Nucl. Mat., 297, 206-213

ICRP (2008). ICRP Publication 107, Nuclear Decay Data for Dosimetric Calculations. Annals of the ICRP, 38(3), International Commission on Radiological Protection.

Jernström, J., Vuorinen, U., Hakanen, M. (2002) Solubility of thorium in 0.1 M NaCl solution and in saline and fresh anoxic reference groundwater, in Report 2002-06

Landesman, C., Delaunay, S., Grambow, B. (2004) Leaching behavior of unirradiated high temperature reactor (HTR) UO_2-ThO_2 mixed oxides fuel particles. Mater. Res. Soc. Symp. Proc., 807

Moon, H.C. (1989) Equilibrium ultrafiltration of hydrolized thorium (IV) solutions. Bull. Korean Chem. Soc., 10, 270-272

Nabivanets, B., Kudritskaya, L.N. (1964) Hydrocomplexes of thorium(IV). Ukr. Khim. Zh., 30, 891-895

Neck, V., Kim, J.I. (2001) Solubility and hydrolysis of tetravalent actinides. Radiochim. Acta, 9, 1-16

Neck, V., Müller, R., Bouby, M., Altmaier, M., Rothe, J., Denecke, M.A., Kim, J.I. (2002) Solubility of amorphous Th(IV) hydroxide - application of LIBD to determine the solubility product and EXAFS for aqueous speciation. Radiochim. Acta, 90, 485-494

Östhols, E. (1995) The solubility of microcrystalline ThO_2 in phosphate media. Radiochim. Acta, 788, 1-6

Östhols, E., Bruno, J., Grenthe, I. (1994) On the influence of carbonate on mineral dissolution: III. The solubility of microcrystalline ThO_2 in CO_2-H_2O media. Geochim. Cosmochim. Acta, 58, 613-623

Quintessa Limited (2011) AMBER 5.5 Reference Guide. QE-AMBER-1, Version 5.5

Rai, D., Felmy, A.R., Sterner, S.M., Moore, D.A., Mason, M.J., Novak, C.F. (1997) The solubility of Th(IV) and U(IV) hydrous oxides in concentrated NaCl anf $MgCl_2$ solutions. Radiochim. Acta, 79, 239-247

Rai, D., Moorw, D.A., Oakes, C.S., Yui, M. (2000) Thermodynamic model for the solubility of thorium dioxide in the Na^+-Cl^--OH^--H_2O system at 23°C and 90°C. Radiochim. Acta, 88, 297-306

Rand, M., Fuger, J., Grenthe, I., Neck, V., Rai, D. (2008) Chemical Thermodynamics of Thorium. book, ed. OECD and NEA. Vol. 11., Amsterdam, The Netherlands: North Holland Elsevier Science Publishers B. V.

Rothe, J., Denecke, M.A., Neck, V., Müller, R., Kim, J.I. (2002) XAFS investigation of the structure of aqueous Thorium(IV) species, colloids, and solid Thorium(IV) oxide/hydroxide. Inorg. Chem., 41, 249-258

Rousseau, G. (2002) Coprécipitation de Th, Eu, La et Ac avec UO_2 comme phase d'accueil, in Ph.D. Université de Nantes: Nantes.

Rousseau, G., Fattahi, M., Grambow, B., Boucher, F., Ouvrard, G. (2002) Coprecipitation of thorium with UO_2. Radiochim. Acta, 90, 523-527

Rousseau, G., Fattahi, M., Grambow, B., Boucher, F., Ouvrard, G. (2006) Coprecipitation of thorium and lanthanum with UO_{2+x}(s) as host phase. Radiochim. Acta, 94, 517-522

Ryan, J.L., Rai, D. (1987) Thorium(IV) hydrous oxide solubility. Inorg. Chem., 26, 4140-4142

Sena, C., Salas, J., Arcos, D. (2010) Aspects of geochemical evolution of the SKB near field in the frame of SR-Site. SKB Technical Report, TR-10-59

SKB (2010a) Data report for the safety assessment SR-Site. SKB Technical Report, TR-10-52

SKB (2010b) Fuel and canister process report for the safety assessment SR-Site. SKB Technical Report, TR-10-46

SKB (2010c) Radionuclide transport report for the safety assessment SR-Site. SKB Technical Report, TR-10-50

SKB (2011) Long-term safety for the final repository for spent nuclear fuel at Forsmark. Main report of the SR-Site project. Volume I. SKB Technical Report, TR-11-01

Vandenborre, J., Abdelouas, A., Grambow, B. (2008) Discrepancies in thorium oxide solubility values: a new experimental approach to improve understanding of oxide surface at solid/solution interface. Radiochim. Acta, 96, 515-520

Wagman, D.D., Evans, W.H, Parker, V.B., Schumm, R.H., Halow, I., Bailey, S.M., Churney, K.L., Nuttall, R.L. (1982) The NBS Tables of Chemical Thermodynamic Properties, Selected Values for Inorganic C_1 and C_2 Organic Substances in SI Units. J. Phys. Chem., 11.

Wierczinski, B., Helfer, S., Ochs, M., Skarnemark, G. (1998) Solubility measurements and sorption studies of thorium in cement pore water. J. Alloys Compd., 271-273, 272-276

Appendix: Selected data

Table 4: Radionuclides of interest, decay rates and inventory

Elements of interest	Isotopes	Decay chain*	Decay rate	Inventory** (mol/canister)
Ac	^{227}Ac	^{227}Ac → ^{227}Th	21.8 y	1.34E-9
	^{228}Ac	^{228}Ac → ^{228}Th	6.2 h	--
Am	^{241}Am	^{241}Am → ^{237}Np	432.2 y	9.21E+0
Cs	^{137}Cs	^{137}Cs → ^{137m}Ba	30.2 y	8.69E+0
Eu	^{152}Eu	^{152}Eu → ^{152}Gd	13.5 y	8.32E-5
Np	^{237}Np	^{237}Np → ^{233}Pa	2.2E+6 y	4.71E+0
Pa	^{231}Pa	^{231}Pa → ^{227}Ac	3.3E+4 y	5.92E-6
	^{234m}Pa	^{234m}Pa → ^{234}U	6.7 h	3.67E-12
Ra	^{223}Ra	^{223}Ra → ^{219}Rn	11.4 d	--
	^{224}Ra	^{224}Ra → ^{220}Rn	3.7 d	--
	^{226}Ra	^{226}Ra → ^{222}Rn	1.6E+3 y	3.03E-8
	^{228}Ra	^{228}Ra → ^{228}Ac	5.8 y	--
Se	^{79}Se	^{79}Se → ^{79}Br	3.0E+5 y	1.36E-1
Sr	^{90}Sr	^{90}Sr → ^{90}Y	28.8 y	5.43E+0
Tc	^{99}Tc	^{99}Tc → ^{99}Ru	2.1E+5 y	1.79E+1
Th	^{227}Th	^{227}Th → ^{223}Ra	18.7 d	--
	^{228}Th	^{228}Th → ^{224}Ra	1.9 y	--
	^{230}Th	^{230}Th → ^{226}Ra	7.5E+4	1.75E-4
	^{231}Th	^{231}Th → ^{231}Pa	25.5 h	--
	^{232}Th	^{232}Th → ^{228}Ra	1.4E+10 y	4.49E-5
	^{234}Th	^{234}Th → ^{234m}Pa	24.1 d	1.07E-7
U	^{234}U	^{234}U → ^{230}Th	2.5E+5 y	1.82E+0
	^{235}U	^{235}U → ^{231}Th	7.0E+8 y	5.76E+1
	^{238}U	^{238}U → ^{234}Th	4.5E+9 y	7.20E+3

* It has been considered all daughters of natural decay chains until the last isotope of interest (^{226}Ra for ^{238}U chain; ^{223}Ra for ^{235}U chain; ^{228}Ra for ^{232}Th chain).

** Waste inventory in mol per average canister at year 2045. The initial amount of all elements in the rest of compartments is assumed to be zero.

Decay rate data from ICRP (2008)

Inventory from SKB (2010a)

Table 5: Compartment dimensions and density

Compartment	Length (m)	Distance to center (m)		Density (kg/m^3)
		Internal	External	
Waste	4.8	0	0.50	--
Canister	4.8	0.50	0.55	8920
		0.55	0.62	
		0.62	0.69	
Bentonite	4.8	0.69	0.76	2000
		0.76	0.83	
		0.83	0.90	
EDZ	4.8	0.90	1.30	2700
		1.30	1.70	
		1.70	2.71	
Granite	4.8	2.71	2.50	2700
		2.50	2.90	
		2.90	3.30	
Sink	4.8	3.30	4.00	--

Length and *radius of material* data from Sena et al. (2010). Discretization internal decision

Density data from SKB (2010a) but canister data from SKB (2010b)

Table 6: IRF and matrix dissolution data

Element	IRF (-)	Dissolution
Ac	0	All radionuclides embedded in UO_2 matrix will be released at the same rate as matrix dissolution. Best estimate: 1E-7 y^{-1}
Am	0	
Cs	0.025	
Eu	0	
Np	0	
Pa	0	
Ra	0	
Se	0.0038	
Sr	0.0025	
Tc	0.002	
Th	0	
U	0	

IRF and *dissolution* data from SKB (2010a)

Table 7: Effective diffusion, sorption coeficient and porosity data in bentonite and granite

Element	Bentonite			Granite		
	$D_{e,m,i}$ (m^2/s)	$K_{d,m,I}$ (m^3/kg)	$\theta_{m,i}$ (%)	$D_{e,m,i}$ (m^2/s)	$K_{d,m,I}$ (m^3/kg)	$\theta_{m,i}$ (%)
Ac	1.4E-10	8	43.5	2.1E-14	1.48E-2	0.18
Am	1.4E-10	61	43.5	2.1E-14	1.48E-2	0.18
Cs	4.2E-10	0.093	43.5	2.1E-14	3.49E-4	0.18
Eu	1.4E-10	8	43.5	2.1E-14	1.48E-2	0.18
Np	1.4E-10	**63, (IV)** 0.02, (V)	43.5	2.1E-14	5.29E-2	0.18
	1.4E-10	3	43.5	2.1E-14	5.29E-2	0.18
Ra	1.4E-10	0.0045	43.5	2.1E-14	2.24E-4	0.18
Se	1.1E-11	**0, (-II, VII)** 0.04, (IV)	17.4	6.6E-15	2.95E-4	0.18
Sr	1.4E-10	0.0045	43.5	2.1E-14	3.42E-6	0.18
Tc	1.4E-10	**60, (IV)** 0, (VII)	43.5	2.1E-14	5.29E-2	0.18
Th	1.4E-10	63	43.5	2.1E-14	5.29E-2	0.18
U	1.4E-10	**63, (IV)** 3, (VI)	43.5	2.1E-14	**5.29E-2 (IV)** 1.06E-4(VI)	0.18

All data from TR-10-52
Selected data for redox sensitive elements in bold (based on TR-06-32)

Table 8: Water flow data

Material	Q (m^3/y)
EDZ Granite	$5 \cdot 10^{-6}$

Water flow data from Sena et al. (2010)

Table 9: Solubility data

Element	Solubility (mol/L)		
	Waste/Canister	Bentonite	EDZ/Granite*
Am	$AmOHCO_3$ $8.7 \cdot 10^{-6}$ **$Am_2(CO_3)_3$ $4.1 \cdot 10^{-6}$**	$AmOHCO_3$ $8.7 \cdot 10^{-6}$ **$Am_2(CO_3)_3$ $4.1 \cdot 10^{-6}$**	$Am_2(CO_3)_2Na \cdot 5H_2O$ $3.0 \cdot 10^{-6}$
Cs	n.s.l	n.s.l	n.s.l
Eu	Eu(OH)3(cr) $4.0 \cdot 10^{-4}$	Eu(OH)3(cr) $4.0 \cdot 10^{-4}$	Eu(OH)3(cr) $4.0 \cdot 10^{-4}$
Np	$NpO_2 \cdot 2H_2O$ $1.0 \cdot 10^{-9}$	$NpO_2 \cdot 2H_2O$ $1.0 \cdot 10^{-9}$	$NpO_2 \cdot 2H_2O$ $1.1 \cdot 10^{-9}$
Pa	Pa_2O_5 $3 \cdot 10^{-7}$	Pa_2O_5 $3 \cdot 10^{-7}$	Pa_2O_5 $3 \cdot 10^{-7}$
Ra	$RaSO_4$ $9.8 \cdot 10^{-8}$	$RaSO_4$ $1.0 \cdot 10^{-7}$	$RaSO_4$ $2.3 \cdot 10^{-7}$
Se	FeSe $1.4 \cdot 10^{-10}$	FeSe $1.4 \cdot 10^{-10}$	FeSe $1.8 \cdot 10^{-11}$
Sr	Celestite $6.7 \cdot 10^{-4}$	Celestite $6.9 \cdot 10^{-4}$	Celestite $9.8 \cdot 10^{-4}$
Tc	$TcO_2 \cdot 1.6H_2O$ $4.4 \cdot 10^{-9}$	$TcO_2 \cdot 1.6H_2O$ $4.4 \cdot 10^{-9}$	$TcO_2 \cdot 1.6H_2O$ $4.3 \cdot 10^{-9}$
Th	$ThO_2 \cdot 2H_2O$ $7.9 \cdot 10^{-7}$	$ThO_2 \cdot 2H_2O$ $7.9 \cdot 10^{-7}$	$ThO_2 \cdot$(am, aged) $8.9 \cdot 10^{-9}$
U	**$UO_2 \cdot 2H_2O$ $9.5 \cdot 10^{-9}$** Uranophane $1.9 \cdot 10^{-6}$ Becquerelite (nat) $3.0 \cdot 10^{-6}$	**$UO_2 \cdot 2H_2O$ $6.8 \cdot 10^{-10}$** $UO_{2.34}$ $1.5 \cdot 10^{-9}$ $UO_{2.25}$ $3.0 \cdot 10^{-11}$	$UO_2 \cdot$(am, aged) $4.2 \cdot 10^{-7}$

Solubility limits from Duro et al. (2006)

*Updated values from Grivé et al. (2010)